ACS OMEGA

http://pubs.acs.org/journal/acsodf

Article

SOMO−HOMO Conversion in Triplet Cyclopentane-1,3-diyl Diradicals

Zhe Wang, Ryo Murata, and Manabu Abe*

Cite This: *ACS Omega* 2021, 6, 22773−22779

Read Online

ACCESS | Metrics & More | Article Recommendations | Supporting Information

ABSTRACT: According to the Aufbau principle, singly occupied molecular orbitals (SOMOs) are energetically higher lying than a highest doubly occupied molecular orbital (HOMO) in the electronically ground state of radicals. However, in the last decade, SOMO−HOMO-converted species have been reported in a limited group of radicals, such as distonic anion radicals and nitroxides. In this study, SOMO−HOMO conversion was observed in triplet 2,2-difluorocyclopentane-1,3-diyl diradicals **DR3F1**, **DR4F1**, and 2-fluorocyclopentante-1,3-diyl diradical **DR3HF1**, which contain the anthracyl unit at the remote position. The high HOMO energy in the anthracyl moiety and the low-lying SOMO−1 due to the fluoro-substituent effect are the key to the SOMO−HOMO conversion phenomenon. Furthermore, the cation radical **DR3F1**$^+$ generated through the one-electron oxidation of **DR3F1** was found to be a SOMO−HOMO-converted monoradical.

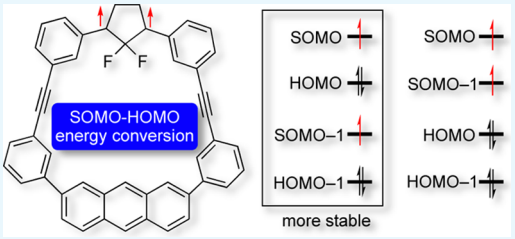

INTRODUCTION

According to the Aufbau principle, singly occupied molecular orbitals (SOMOs) have a higher energy than doubly occupied molecular orbitals in the most stable electronic configuration of ground-state molecules. However, SOMO−highest occupied molecular orbital (HOMO)-converted molecules, in which the SOMO has a lower energy than the HOMO, have been reported in radicals such as metal complexes,[1,2] distonic anion radicals,[3−9] nitroxides,[10−12] and some stable tris(2,4,6-trichlorophenyl)methyl derivatives.[13,14] The generation of high-spin molecules from monoradicals through oxidation and the switching of bond dissociation energy are of particular interest in the chemistry of SOMO−HOMO-converted molecules. Although the reactivity of SOMO−HOMO-converted molecules has attracted considerable attention in radical chemistry, only a limited number of organic molecules have been reported to date. Recently, SOMO−HOMO-converted triplet carbenes have been found by this laboratory.[15] The search for molecules that undergo SOMO−HOMO conversion will advance the field of radical chemistry.

A long-lived diradical, **DR1**,[16] was reported in a macrocyclic system that involves the naphthyl moiety at a remote position from the diradical unit (Figure 1a). In its triplet state, the HOMO is not located in the benzene rings adjacent to the diradical unit but mainly in the naphthyl moiety (Figure 1b). The HOMO is in the benzene ring of the triplet diradical **DR2**[17] without the macrocyclic ring system. Two SOMOs, ψ_S and ψ_A, of T-**DR1** were calculated to be higher in energy than the HOMO of the naphthyl group at the UB3LYP/6-31G(d)[18−20] level of theory, following the Aufbau principle (Figure 1b). As SOMOs and HOMO parts are in separate positions, it is possible to generate SOMO−HOMO-converted triplet diradicals by increasing the energy of the HOMO and/or decreasing the energy of the SOMOs. In this study, the effects of substituent X and ring size *n* of the aromatic moiety at the remote position on the SOMO−HOMO conversion phenomenon in the triplet diradical **DR3** were investigated. To understand the macrocyclic effect, the substituent and aromatic ring effects were also examined in the linearly substituted diradical **DR4**.

RESULTS AND DISCUSSION

First, the molecular structure of the triplet states of **DR3** (X = H, F; *n* = 0, 1) was optimized in the C_S symmetry at the UB3LYP/6-31G(d) level of theory within the Gaussian 16[21] package. Intriguingly, the SOMO−HOMO conversion, ...(SOMO−1, ψ_S)^1(HOMO)^2(SOMO, ψ_A)^1..., was observed for the difluoro-substituted triplet diradical **DR3F1** (X = F, *n* = 1), featuring the anthracyl unit (Figure 2d), although **DR3H1** (X = H, *n* = 1) and naphthyl-substituted diradicals **DR3H0** (X = H, *n* = 0) and **DR3F0** (X = F, *n* = 0) have a common electronic configuration that follows the Aufbau principle (Figure 2a−c). The aromatic moiety in the macrocyclic system was bent with a bending angle (θ, Figure 1a) of 162.94 and 175.16° in **DR3F1** and **DR3F0**, respectively. As shown in

Received: June 14, 2021
Accepted: July 22, 2021
Published: August 24, 2021

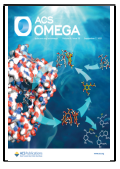

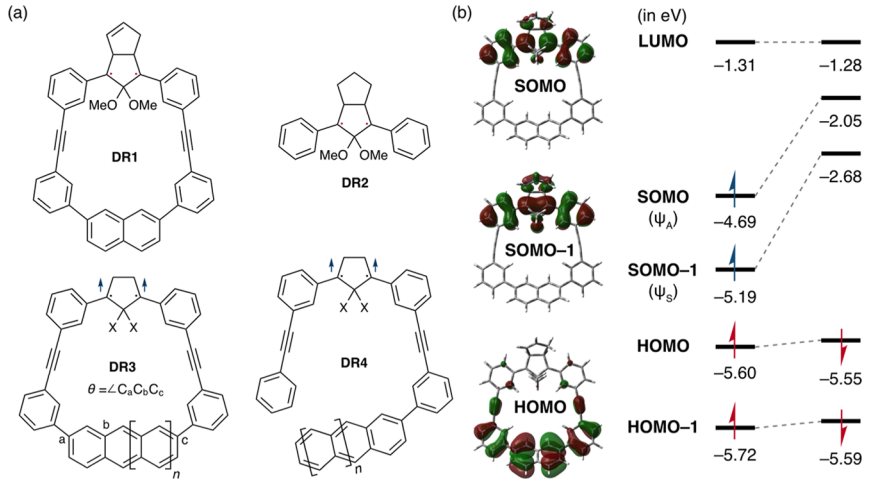

Figure 1. (a) Molecular structures of **DR1**-**4** and (b) molecular orbital diagram of triplet T-**DR1**.

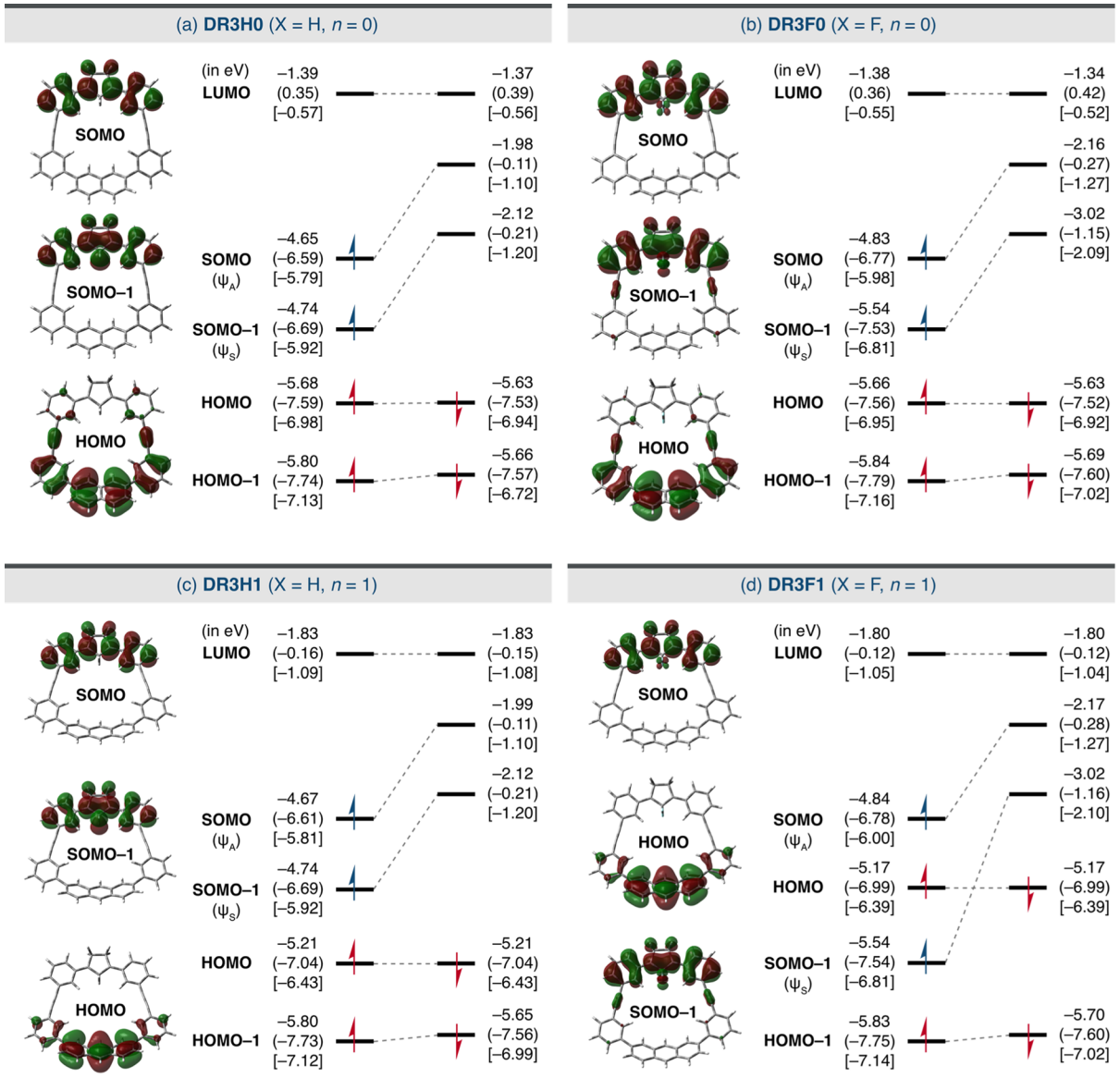

Figure 2. Molecular orbital diagrams of (a) **DR3H0**, (b) **DR3F0**, (c) **DR3H1**, and (d) **DR3F1**. Molecular orbital energies are calculated at the UB3LYP (UωB97X-D) [UM06-2X]/6-31G(d) level of theory.

https://doi.org/10.1021/acsomega.1c03125
ACS Omega 2021, 6, 22773−22779

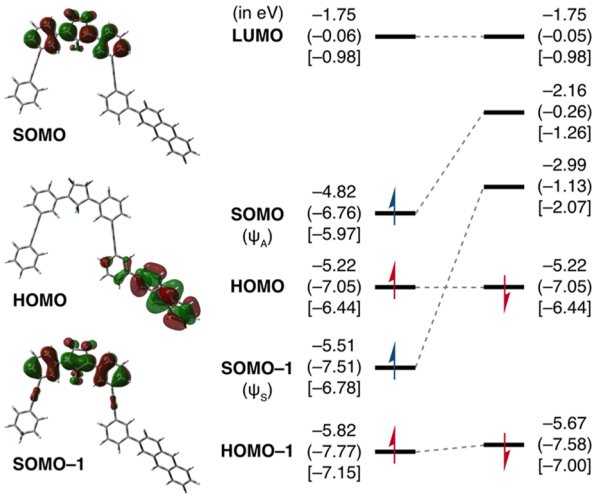

Figure 3. Molecular orbital diagram of **DR4F1**. Molecular orbital energies are calculated at the UB3LYP (UωB97X-D) [UM06-2X]/6-31G(d) level of theory.

Figure 2d, the two SOMOs (ψ_A and ψ_S) are delocalized over the 1,3-diphenylcyclopentane-1,3-diyl unit but do not extend to the anthracyl moiety. The HOMO is mainly localized at the anthracyl moiety, with minor extension to the adjacent phenyl rings. The energy level of SOMO−1 (ψ_S) is approximately 0.37 eV lower than that of the doubly occupied HOMO at the UB3LYP/6-31G(d) level of theory.

In the triplet state of **DR3H1** (X = H, n = 1, Figure 2c), two SOMOs, ψ_S and ψ_A, were higher in energy than the HOMOs by 0.47 and 0.54 eV, respectively. In **DR3H0** and **DR3F0**, the HOMOs have large contribution from the naphthyl unit (θ = 175.17/175.16°), which are approximately 0.94 and 0.12 eV lower in energy than the corresponding SOMO − 1s (ψ_S). The HOMO energies located at the naphthyl moiety were −5.68 and −5.66 eV in **DR3H0** and **DR3F0**, respectively, which are lower by −0.47 and −0.49 eV than those at the anthracyl moiety in **DR3H1** and **DR3F1**, respectively.

To understand the effect of the curved anthracyl moiety on the SOMO−HOMO conversion, the non-macrocyclic diradical **DR4F1** (X = F, n = 1) was computed at the same level of theory (Figure 3). The SOMO−HOMO conversion was also found to occur in **DR4F1**, although the planar anthracyl moiety (θ = 179.92°) gave a lower HOMO energy than that in **DR3F1** by 0.05 eV. Thus, the structure of the anthracyl moiety with a high HOMO energy level and the fluoro group are key

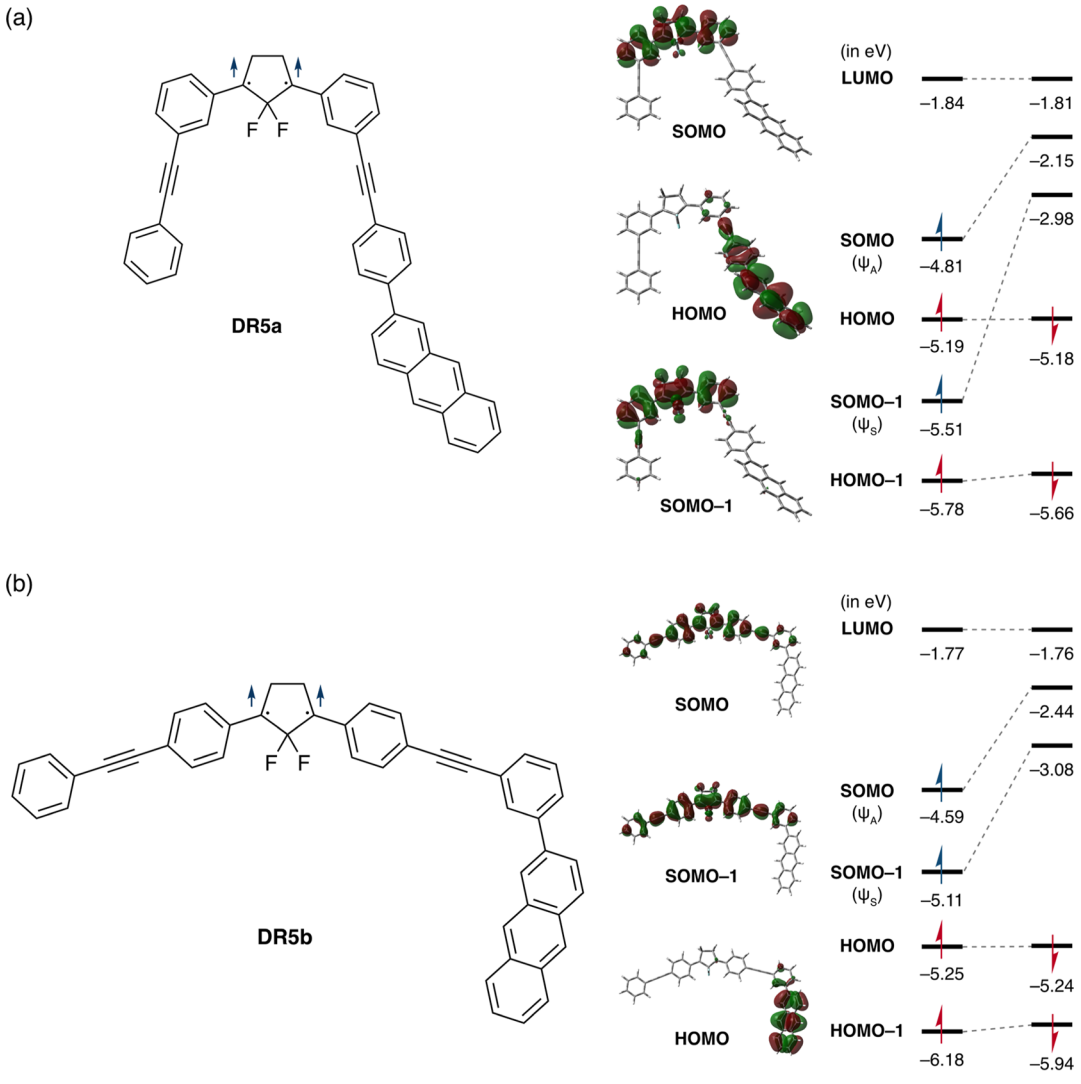

Figure 4. Structure and molecular orbital diagrams of (a) **DR5a** and (b) **DR5b** calculated at the UB3LYP/6-31G(d) level of theory.

https://doi.org/10.1021/acsomega.1c03125
ACS Omega 2021, 6, 22773−22779

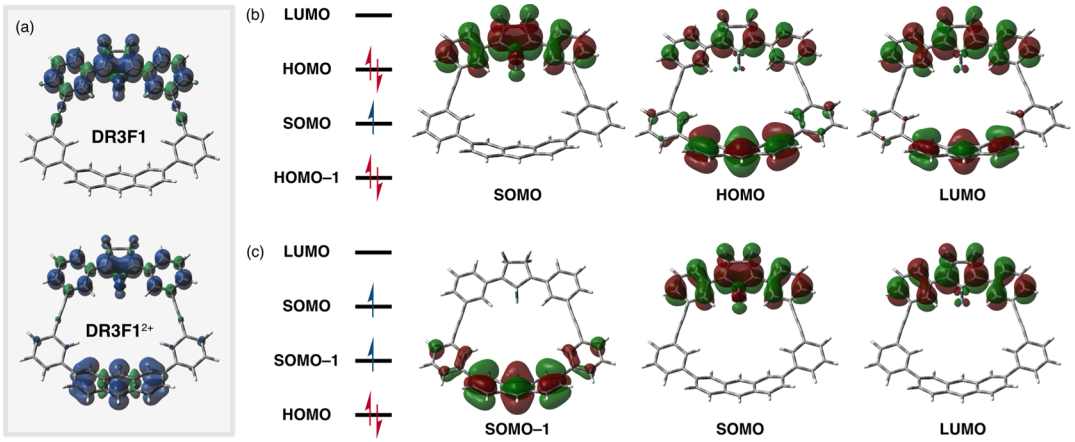

Figure 5. (a) Spin density maps of **DR3F1** and **DR3F1**$^{2+}$. Molecular orbital diagrams of (b) **DR3F1**$^{+}$ and (c) **DR3F1**$^{2+}$.

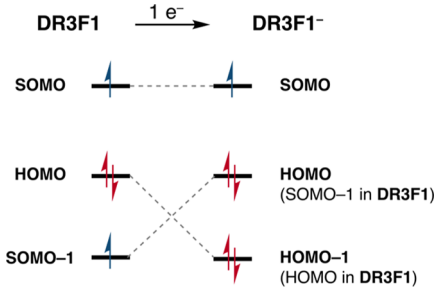

Figure 6. Configurational change of molecular orbitals upon one-electron reduction of **DR3F1** to **DR3F1**$^{-}$.

for the SOMO−HOMO conversion. The slightly higher HOMO energy in **DR3F1** than that in **DR4F1** is explained by the curved structure of the anthryl unit in **DR3F1**. A similar curve effect was reported for cycloparaphenylene compounds.[22−24]

To understand the effect of the *meta*-linkage on the SOMO−HOMO conversion, which decouples the conjugation between the 1,3-diphenyl unit and the anthracyl part, triplet diradicals **DR5a,b** were computed at the same level of theory (Figure 4). The SOMO−HOMO conversion was also observed in **DR5a** having the anthracyl unit connected with the phenyl ring at the *para*-position (Figure 4a), indicating that the linkage pattern of the anthracyl unit does not affect the SOMO−HOMO conversion phenomenon. On the other hand, triplet diradical **DR5b**, in which the 2-(3-anthracylphenyl)-ethynyl unit is connected at the *para*-position with the 1,3-diphenyl part, showed a different behavior. The SOMO−1 was destabilized by the π-conjugation with the ethynylphenyl unit to locate the energy to −5.11 eV, resulting in the disappearance of the SOMO−HOMO conversion in **DR5b** (Figure 4b).

To confirm the density function dependency of the SOMO−HOMO conversion, similar computational studies were also conducted at the long-range correlated density functional theory (LC-DFT) using ωB97X-D[25] and M06-2X[26] functionals with the 6-31G(d) basis set. The orbital energies at UωB97X-D and UM06-2X are shown in parentheses and square brackets, respectively, in Figures 2 and 3. Although the absolute values are different in energies by the DFT methods, the relative energy differences are nearly the same. For example, SOMO−1 was computed to be lower in energy than the HOMO by 0.37, 0.55, and 0.42 eV at the UB3LYP,

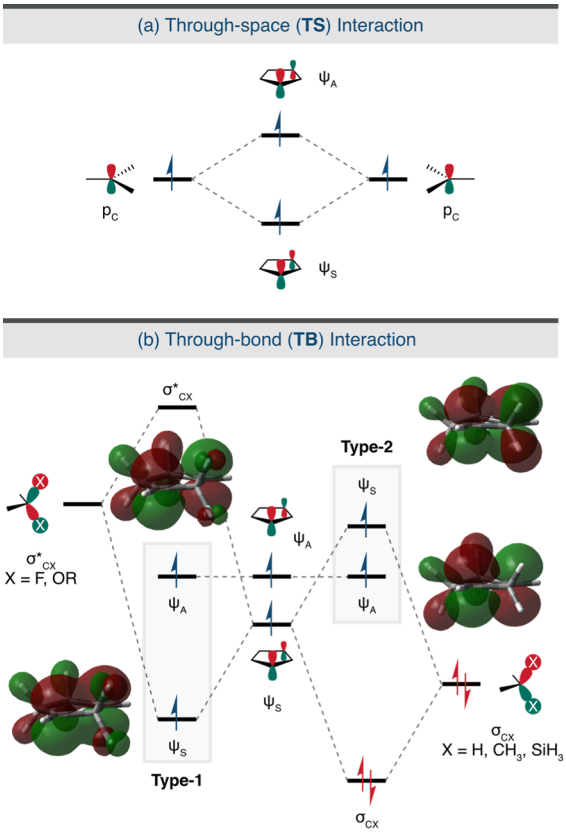

Figure 7. Most stable electronic configuration of the triplet state of cyclopentane-1,3-diyl diradicals: (a) through-space (TS) interaction between two p orbitals in cyclopentane-1,3-diyl. (b) Effect of through-bond (TB) interaction on the relative energy level of ψ_S and ψ_A, left: type-1 (X = F, OR); right: type-2 (X = H, CH_3, and SiR_3).

UωB97X-D, and UM06-2X functionals with the 6-31G(d) basis set, respectively. Thus, the SOMO−HOMO conversion phenomena in **DR3F1** and **DR4F1** were not dependent on the DFT method. In addition to checking the density function dependency, the restricted open-shell (RO) method was tested in computation of the triplet state of **DR3F1**. All the doubly occupied orbitals were found to be lower in energy than the singly occupied orbitals (SOMOs). The total electronic energy at the ROB3LYP/6-31G(d) level of theory was higher in energy by 14.2 kJ mol^{-1} than that at the UB3LYP/6-31G(d) level of theory.

https://doi.org/10.1021/acsomega.1c03125
ACS Omega 2021, 6, 22773−22779

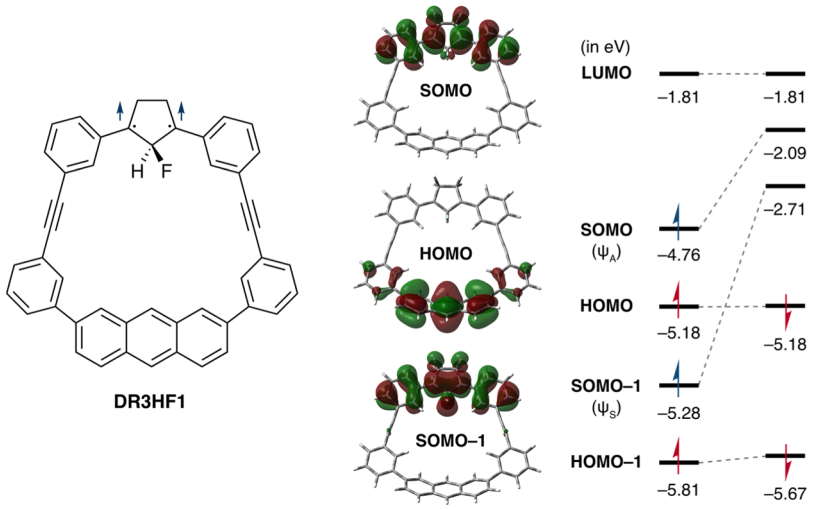

Figure 8. Structure and molecular orbital diagrams of **DR3HF1** calculated at the UB3LYP/6-31G(d) level of theory.

Furthermore, the charged species (radical cation, dication, and radical anion) of the SOMO−HOMO-converted species **DR3F1** were investigated at the UB3LYP/6-31G(d) level of theory. First, the one-electron oxidized cation of **DR3F1**, **DR3F1**$^{+}$, was optimized (Figure 5). The MO analyses showed that **DR3F1**$^{+}$ is also a SOMO−HOMO-converted radical cation (Figure 5b). The singly occupied SOMO is lower lying than the doubly occupied HOMO. The antibonding ψ_A orbital in the cyclopentane unit and the anthracyl moiety contributed to the HOMO and LUMO (Figure 5b). The two-electron oxidation state, the dication **DR3F1**$^{2+}$, was found to be an open-shell diradical species (the wave function is stable at unrestricted calculation, $\Delta E_{CS\text{-}T}$ = 52.57 kJ mol^{-1}). Two singly occupied orbitals were located at the bonding ψ_S orbital in the cyclopentane unit and the anthracyl moiety, both of which are higher in energy than the doubly occupied HOMO (Figure 5c). The spin density map of triplet **DR3F1**$^{2+}$ clearly showed two parallel spins located at the cyclopentane unit and the anthracyl moiety (Figure 5a, bottom), in contrast to the SOMO−HOMO-converted **DR3F1** featuring the two spins at the cyclopentane unit (Figure 5a, up). The radical anion of **DR3F1**, **DR3F1**$^{-}$, was calculated at the UB3LYP/6-31G+(d)[27] level of theory. The use of diffuse functions is essential for predicting the property of anionic species.[28] The normal electronic configuration was found for **DR3F1**$^{-}$. Upon one-electron reduction, the SOMO−1 in **DR3F1** was doubly occupied and became the HOMO in **DR3F1**$^{-}$ (Figure 6).

As mentioned above, the most stable electronic configuration of localized triplet cyclopentane-1,3-diyl diradicals is largely dependent on substituent X and ring size *n*. The energy levels of the two SOMOs, ψ_S and ψ_A, in diradicals are determined by the balance between the through-space (TS) interaction (Figure 7a) of two p orbitals and the through-bond (TB) interaction (Figure 7b) at the C2 position.[29] Because of the TS interaction, the symmetric orbital ψ_S has lower energy than the antisymmetric orbital ψ_A (Figure 7a). In the type-1 molecules (X = electron-withdrawing groups such as F and OR), the TB interaction of ψ_S with the low-lying σ^*_{CX} energetically stabilizes ψ_S, thereby increasing the energy spacing with ψ_A (Figure 7b, left). In contrast, the TB interaction with the high-lying σ_{CX} (X = electron-donating groups such as H, CH_3, and SiR_3) energetically destabilizes ψ_S, thereby switching the energy relationship between ψ_S and ψ_A (type-2, Figure 7b, right). As the diradical **DR3F1** belongs to the type-1 diradical, the SOMO with the symmetric combination (ψ_S) is largely stabilized by the TB interaction. Thus, SOMO−1 in **DR3F1** is lower in energy by 0.80 eV than that in **DR3H1**, which is one of the reasons why the fluoro-substituted **DR3F1** undergoes the SOMO−HOMO conversion in the most stable electronic configuration of the triplet state. The stabilization of ψ_S has also been confirmed in mono-fluoro substituted **DR3HF1** (X = H, X′ = F, *n* = 1), whose ψ_S was lying below the ψ_A by 0.52 eV (Figure 8). Although the energy of SOMO−1 in **DR3HF1** increased by 0.26 eV than that in **DR3F1** due to the weaker type-1 TB interaction, **DR3HF1** also exhibited SOMO−HOMO conversion.

CONCLUSIONS

In the present study, the SOMO−HOMO conversion was observed in triplet cyclopentane-1,3-diyl diradicals. The triplet diradicals **DR3F1** (X = F, *n* = 1) and **DR4F1** (X = F, *n* = 1) adapted the SOMO−HOMO-converted electronic configuration with a high HOMO energy in the anthracyl moiety and low-lying SOMO−1 because of the difluoro-substituent effect. The one-electron oxidation product of **DR3F1**, **DR3F1**$^{+}$, also imparted SOMO−HOMO-converted properties. In contrast, aromatic moieties with lower HOMO energies, such as naphthyl and dihydro-substituted triplet diradicals **DR3H0** and **DR3F0**, follow the Aufbau principle. The *para*-linked derivatives **DR5b** did not show the SOMO−HOMO conversion resulted from alteration in the conjugation pattern.

ASSOCIATED CONTENT

Supporting Information

The Supporting Information is available free of charge at https://pubs.acs.org/doi/10.1021/acsomega.1c03125.

Molecular orbital diagrams; spin density maps; and Cartesian coordinates of computed systems (PDF)

AUTHOR INFORMATION

Corresponding Author

Manabu Abe − *Department of Chemistry, Graduate School of Science, Hiroshima University, Higashi-Hiroshima, Hiroshima 739-8526, Japan; Hiroshima University Research*

https://doi.org/10.1021/acsomega.1c03125
ACS Omega 2021, 6, 22773−22779

Center for Photo-Drug-Delivery-System (HiU-P-DDS), Hiroshima University, Higashi-Hiroshima, Hiroshima 739-8526, Japan; orcid.org/0000-0002-2013-4394; Email: mabe@hiroshima-u.ac.jp

Authors

Zhe Wang − *Department of Chemistry, Graduate School of Science, Hiroshima University, Higashi-Hiroshima, Hiroshima 739-8526, Japan;* orcid.org/0000-0002-9996-586X

Ryo Murata − *Department of Chemistry, Graduate School of Science, Hiroshima University, Higashi-Hiroshima, Hiroshima 739-8526, Japan*

Complete contact information is available at: https://pubs.acs.org/10.1021/acsomega.1c03125

Notes

The authors declare no competing financial interest.

■ ACKNOWLEDGMENTS

This work was supported by the JSPS KAKENHI grant number 21H01921 (M.A.).

■ REFERENCES

(1) Filatov, M.; Harris, N.; Shaik, S. On the "Rebound" Mechanism of Alkane Hydroxylation by Cytochrome P450: Electronic Structure of the Intermediate and the Electron Transfer Character in the Rebound Step. *Angew. Chem., Int. Ed.* **1999**, *38*, 3510−3512.

(2) Westcott, B. L.; Gruhn, N. E.; Michelsen, L. J.; Lichtenberger, D. L. Experimental Observation of Non-Aufbau Behavior: Photoelectron Spectra of Vanadyloctaethylporphyrinate and Vanadylphthalocyanine. *J. Am. Chem. Soc.* **2000**, *122*, 8083−8084.

(3) Gryn'ova, G.; Coote, M. L. Origin and Scope of Long-Range Stabilizing Interactions and Associated SOMO−HOMO Conversion in Distonic Radical Anions. *J. Am. Chem. Soc.* **2013**, *135*, 15392−15403.

(4) Gryn'ova, G.; Marshall, D. L.; Blanksby, S. J.; Coote, M. L. Switching Radical Stability by pH-Induced Orbital Conversion. *Nat. Chem.* **2013**, *5*, 474−481.

(5) Franchi, P.; Mezzina, E.; Lucarini, M. SOMO−HOMO Conversion in Distonic Radical Anions: An Experimental Test in Solution by EPR Radical Equilibration Technique. *J. Am. Chem. Soc.* **2014**, *136*, 1250−1252.

(6) Kumar, A.; Sevilla, M. D. Proton Transfer Induced SOMO-to-HOMO Level Switching in One-Electron Oxidized A-T and G-C Base Pairs: A Density Functional Theory Study. *J. Phys. Chem. B* **2014**, *118*, 5453−5458.

(7) Kumar, A.; Sevilla, M. D. SOMO−HOMO Level Inversion in Biologically Important Radicals. *J. Phys. Chem. B* **2018**, *122*, 98−105.

(8) So, S.; Kirk, B. B.; Wille, U.; Trevitt, A. J.; Blanksby, S. J.; da Silva, G. Reactions of a Distonic Peroxyl Radical Anion Influenced by SOMO−HOMO Conversion: An Example of Anion-Directed Channel Switching. *Phys. Chem. Chem. Phys.* **2020**, *22*, 2130−2141.

(9) Kasemthaveechok, S.; Abella, L.; Jean, M.; Cordier, M.; Roisnel, T.; Vanthuyne, N.; Guizouarn, T.; Cador, O.; Autschbach, J.; Crassous, J.; Favereau, L. Axially and Helically Chiral Cationic Radical Bicarbazoles: SOMO−HOMO Level Inversion and Chirality Impact on the Stability of Mono- and Diradical Cations. *J. Am. Chem. Soc.* **2020**, *142*, 20409−20418.

(10) Kusamoto, T.; Kume, S.; Nishihara, H. Realization of SOMO−HOMO Level Conversion for a TEMPO-Dithiolate Ligand by Coordination to Platinum(II). *J. Am. Chem. Soc.* **2008**, *130*, 13844−13845.

(11) Kusamoto, T.; Kume, S.; Nishihara, H. Cyclization of TEMPO Radicals Bound to Metalladithiolene Induced by SOMO−HOMO Energy-Level Conversion. *Angew. Chem., Int. Ed.* **2010**, *49*, 529−531.

(12) Sugawara, T.; Komatsu, H.; Suzuki, K. Interplay between Magnetism and Conductivity Derived from Spin-Polarized Donor Radicals. *Chem. Soc. Rev.* **2011**, *40*, 3105−3118.

(13) Tanushi, A.; Kimura, S.; Kusamoto, T.; Tominaga, M.; Kitagawa, Y.; Nakano, M.; Nishihara, H. NIR Emission and Acid-Induced Intramolecular Electron Transfer Derived from a SOMO−HOMO Converted Non-Aufbau Electronic Structure. *J. Phys. Chem. C* **2019**, *123*, 4417−4423.

(14) Guo, H.; Peng, Q.; Chen, X.-K.; Gu, Q.; Dong, S.; Evans, E. W.; Gillett, A. J.; Ai, X.; Zhang, M.; Credgington, D.; Coropceanu, V.; Friend, R. H.; Brédas, J.-L.; Li, F. High Stability and Luminescence Efficiency in Donor−Acceptor Neutral Radicals not Following the Aufbau Principle. *Nat. Mater.* **2019**, *18*, 977−984.

(15) Murata, R.; Wang, Z.; Miyazawa, Y.; Antol, I.; Yamago, S.; Abe, M. SOMO−HOMO Conversion in Triplet Carbenes. *Org. Lett.* **2021**, *23*, 4955−4959.

(16) Wang, Z.; Akisaka, R.; Yabumoto, S.; Nakagawa, T.; Hatano, S.; Abe, M. Impact of the Macrocyclic Structure and Dynamic Solvent Effect on the Reactivity of a Localised Singlet Diradicaloid with π-Single Bonding Character. *Chem. Sci.* **2021**, *12*, 613−625.

(17) Nakagaki, T.; Sakai, T.; Mizuta, T.; Fujiwara, Y.; Abe, M. Kinetic Stabilization and Reactivity of π Single-Bonded Species: Effect of the Alkoxy Group on the Lifetime of Singlet 2,2-Dialkoxy-1,3-diphenyloctahydropentalene-1,3-diyls. *Chem.—Eur. J.* **2013**, *19*, 10395−10404.

(18) Becke, A. D. Density-Functional Thermochemistry. III. The Role of Exact Exchange. *J. Chem. Phys.* **1993**, *98*, 5648−5652.

(19) Hehre, W. J.; Ditchfield, R.; Pople, J. A. Self−Consistent Molecular Orbital Methods. XII. Further Extensions of Gaussian−Type Basis Sets for Use in Molecular Orbital Studies of Organic Molecules. *J. Chem. Phys.* **1972**, *56*, 2257−2261.

(20) Hariharan, P. C.; Pople, J. A. The Influence of Polarization Functions on Molecular Orbital Hydrogenation Energies. *Theor. Chim. Acta* **1973**, *28*, 213−222.

(21) Frisch, M. J.; Trucks, G. W.; Schlegel, H. B.; Scuseria, G. E.; Robb, M. A.; Cheeseman, J. R.; Scalmani, G.; Barone, V.; Petersson, G. A.; Nakatsuji, H.; Li, X.; Caricato, M.; Marenich, A. V.; Bloino, J.; Janesko, B. G.; Gomperts, R.; Mennucci, B.; Hratchian, H. P.; Ortiz, J. V.; Izmaylov, A. F.; Sonnenberg, J. L.; Williams-Young, D.; Ding, F.; Lipparini, F.; Egidi, F.; Goings, J.; Peng, B.; Petrone, A.; Henderson, T.; Ranasinghe, D.; Zakrzewski, V. G.; Gao, J.; Rega, N.; Zheng, G.; Liang, W.; Hada, M.; Ehara, M.; Toyota, K.; Fukuda, R.; Hasegawa, J.; Ishida, M.; Nakajima, T.; Honda, Y.; Kitao, O.; Nakai, H.; Vreven, T.; Throssell, K.; Montgomery, J. A., Jr.; Peralta, J. E.; Ogliaro, F.; Bearpark, M. J.; Heyd, J. J.; Brothers, E. N.; Kudin, K. N.; Staroverov, V. N.; Keith, T. A.; Kobayashi, R.; Normand, J.; Raghavachari, K.; Rendell, A. P.; Burant, J. C.; Iyengar, S. S.; Tomasi, J.; Cossi, M.; Millam, J. M.; Klene, M.; Adamo, C.; Cammi, R.; Ochterski, J. W.; Martin, R. L.; Morokuma, K.; Farkas, O.; Foresman, J. B.; Fox, D. J. *Gaussian 16*, Revision B.01; Gaussian, Inc.: Wallingford CT, 2016.

(22) Iwamoto, T.; Watanabe, Y.; Sakamoto, Y.; Suzuki, T.; Yamago, S. Selective and Random Syntheses of [n]Cycloparaphenylenes (*n* = 8−13) and Size Dependence of Their Electronic Properties. *J. Am. Chem. Soc.* **2011**, *133*, 8354−8361.

(23) Miyazawa, Y.; Wang, Z.; Matsumoto, M.; Hatano, S.; Antol, I.; Kayahara, E.; Yamago, S.; Abe, M. 1,3-Diradicals Embedded in Curved Paraphenylene Units: Singlet versus Triplet State and In-Plane Aromaticity. *J. Am. Chem. Soc.* **2021**, *143*, 7426−7439.

(24) Darzi, E. R.; Jasti, R. The Dynamic, Size-Dependent Properties of [5]-[12]Cycloparaphenylenes. *Chem. Soc. Rev.* **2015**, *44*, 6401−6410.

(25) Chai, J.-D.; Head-Gordon, M. Long-Range Corrected Hybrid Density Functionals with Damped Atom−Atom Dispersion Corrections. *Phys. Chem. Chem. Phys.* **2008**, *10*, 6615−6620.

(26) Zhao, Y.; Truhlar, D. G. The M06 Suite of Density Functionals for Main Group Thermochemistry, Thermochemical Kinetics, Noncovalent Interactions, Excited States, and Transition Elements: Two New Functionals and Systematic Testing of Four M06-Class

Functionals and 12 Other Functionals. *Theor. Chem. Acc.* **2008**, *120*, 215−241.
(27) Clark, T.; Chandrasekhar, J.; Spitznagel, G. W.; Schleyer, P. V. R. Efficient diffuse function-augmented basis sets for anion calculations. III. The 3-21+G basis set for first-row elements, Li−F. *J. Comput. Chem.* **1983**, *4*, 294−301.
(28) Woon, D. E.; Dunning, T. H. Gaussian basis sets for use in correlated molecular calculations. III. The atoms aluminum through argon. *J. Chem. Phys.* **1993**, *98*, 1358−1371.
(29) Abe, M. Diradicals. *Chem. Rev.* **2013**, *113*, 7011−7088.

https://doi.org/10.1021/acsomega.1c03125
ACS Omega 2021, 6, 22773−22779